Sensors & Diagnostics

Accepted Manuscript

This article can be cited before page numbers have been issued, to do this please use: N. Chettri, H. V. Barkale, S. Jha and N. Dey, *Sens. Diagn.*, 2026, DOI: 10.1039/D6SD00054A.

DOI: 10.1039/D6SD00054A

Structure-Guided Aggregation-Regulated and Coordination-Assisted Zn–Porphyrins for Decoding Aminoglycoside Recognition in Real-Life Samples

Nisha Chettri,[a±] Harshal V Barkale,[b±] Satadru Jha,[a] Nilanjan Dey[b*]

[a] Department of Chemistry, Sikkim Manipal Institute of Technology, Sikkim Manipal University, Majitar, Sikkim 737136, India.

[b] Department of Chemistry, BITS-Pilani Hyderabad Campus, Shameerpet, Hyderabad-500078, Telangana, India, *Email: nilanjandey.iisc@gmail.com

±Both the authors contributed equally to this work

ABSTRACT

Herein, we report an aggregation-regulated Zn–porphyrin–based optical sensing platform for the selective detection of the aminoglycoside antibiotic neomycin in aqueous media and real-life samples. Three structurally related Zn–porphyrin derivatives with systematically varied peripheral substituents were designed to modulate supramolecular aggregation behavior and accessibility of the Zn^{2+} center. Comparative photophysical studies revealed that an optimal balance between aggregation and steric accessibility is essential for efficient sensing, with compound 1 exhibiting the most pronounced response. Neomycin binding triggered coordination-assisted and electrostatic reorganization of porphyrin aggregates, leading to a characteristic ratiometric fluorescence response involving quenching of the native porphyrinic emission and emergence of a distinct blue-shifted band at ~475 nm. The mechanistic investigations established aggregation modulation as the dominant transduction mechanism, driven largely by favorable entropic contributions. The sensing platform enabled quantitative neomycin detection with a low-micromolar limit of detection (0.75 μM) in complex matrices such as milk, as well as accurate analysis of pharmaceutical formulations. Furthermore, translation of the system onto cellulose-based paper strips afforded a low-cost, portable, and instrument-free detection tool. The novelty of this work lies in establishing a systematic structure–aggregation–response correlation in Zn–porphyrin systems, where controlled peripheral modification governs aggregation behavior and Zn^{2+} accessibility, enabling preferential sensing of neomycin through coordination-assisted modulation of supramolecular assemblies.

KEYWORDS: Metalloporphyrins; Aminoglycoside Antibiotics, Emerging Contaminants; Fluorescence response; Self-Assembly; Real-life Samples

INTRODUCTION

The detection of emerging contaminants in water systems has become a critical scientific and technological challenge due to their continuous release, chemical persistence, and potential long-term impacts on human health and aquatic ecosystems, even at trace concentrations.[1, 2]

View Article Online
DOI: 10.1039/D6SD00054A

These contaminants, including antibiotics, pharmaceuticals, personal care products, endocrine disruptors, and other biologically active agents are typically present at ng–μg L^{-1} levels and coexist with complex aqueous matrices enriched with natural organic matter, dissolved salts, and competing ions, which severely complicates reliable detection and quantification. Conventional analytical techniques such as HPLC, GC–MS, and LC–MS/MS provide excellent sensitivity and molecular specificity; however, they are infrastructure-intensive, time-consuming, costly, and largely unsuitable for real-time, in situ, or decentralized monitoring. [3] Optical and chemical sensing platforms offer attractive alternatives owing to their rapid response, operational simplicity, high sensitivity, and portability, yet they still face persistent challenges, including signal drift, surface fouling, cross-reactivity, limited robustness under fluctuating pH, temperature, and ionic strength, and inefficient transduction of weak analyte-sensor interactions into quantifiable outputs.[4] Addressing these limitations necessitates sensing strategies that integrate selective molecular recognition with intrinsic signal amplification mechanisms, such as aggregation or interfacial modulation, while maintaining strong tolerance toward complex sample matrices.[5]

Among the diverse classes of emerging contaminants, aminoglycoside antibiotics represent a particularly important and challenging subgroup requiring both sensitive detection and reliable discrimination.[6] Aminoglycosides such as neomycin, kanamycin, gentamicin, and streptomycin are extensively employed in clinical medicine, veterinary practice, and animal husbandry due to their broad-spectrum antibacterial activity and high efficacy against Gram-negative pathogens. [7] Their high polarity, multiple amino functionalities, and poor metabolic degradation contribute to significant environmental persistence and frequent occurrence in aquatic systems, where even trace-level residues can promote antimicrobial resistance and disrupt microbial ecosystems. From a health perspective, prolonged or uncontrolled exposure to aminoglycosides is associated with severe adverse effects, including nephrotoxicity, ototoxicity, and neuromuscular toxicity, underscoring the need for stringent monitoring in food products, pharmaceutical formulations, and environmental samples.[8] Technically, discrimination among aminoglycosides remains challenging because of their closely related molecular frameworks and similar chromatographic, electrochemical, and spectroscopic signatures, necessitating sensing platforms capable of both low-level detection and structural differentiation.

View Article Online
DOI: 10.1039/D6SD00054A

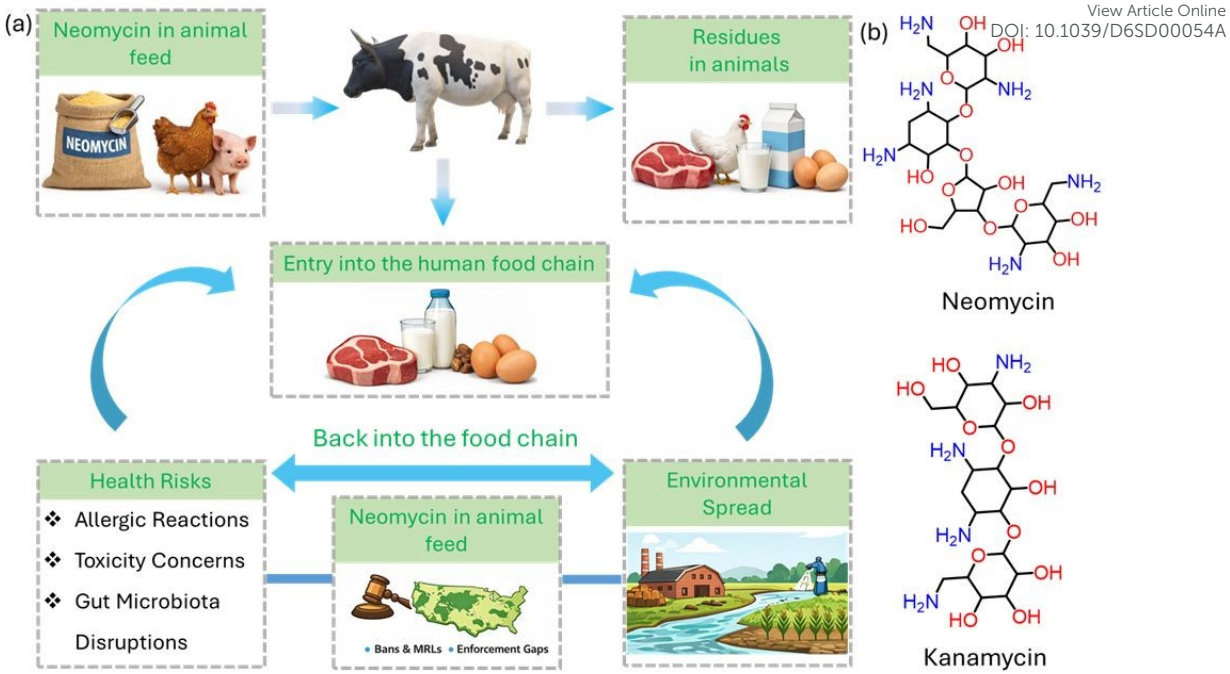

Figure 1. (a) The schematic diagram shows the source of neomycin in food samples (b) Structure of Neomycin and Kanamycin (aminoglycoside antibiotics)

In this context, the present work addresses the fundamental challenge of selective detection and discrimination of aminoglycoside antibiotics in aqueous environments by exploiting aggregation-regulated photophysics of Zn–porphyrins. The study was guided by key questions concerning how peripheral structural modulation governs supramolecular aggregation in water, how such aggregates can be selectively reconfigured by aminoglycoside binding, and how these processes can be harnessed to generate amplified and selective optical responses. Three structurally related Zn–porphyrin complexes were rationally designed to systematically tune steric bulk and hydrophobicity, thereby controlling aggregation strength and accessibility of the Zn^{2+} coordination center. The results demonstrate that neomycin induces a unique coordination-assisted reorganization of porphyrin aggregates, producing a distinct ratiometric fluorescence signature characterized by quenching of native porphyrinic emission and emergence of a blue-shifted emissive band (~475 nm), enabling selective detection at low micromolar concentrations even in complex matrices. By combining quantitative mechanistic insight with real-sample analysis and translation to low-cost, paper-based platforms, this work establishes aggregation as an active and tunable transduction element rather than a limitation. The central novelty lies in leveraging structure-directed aggregation modulation of metalloporphyrins to achieve selective aminoglycoside sensing, offering both mechanistic depth and a practical, field-deployable strategy for monitoring emerging antibiotic contaminants.

View Article Online
DOI: 10.1039/D6SD00054A

RESULTS AND DISCUSSION

Design and Synthesis of Metalloporphyrin: The three porphyrin precursors were synthesized via a conventional acid-catalysed condensation of pyrrole with appropriately substituted aldehydes, followed by oxidative aromatization under controlled conditions to afford the corresponding free-base porphyrins.[9] Structural variation at the meso-positions was introduced through the choice of aldehyde precursors, enabling systematic modulation of steric bulk and hydrophobicity in the resulting porphyrin frameworks. The three Zn-porphyrin derivatives (1-3) were synthesized (Figure 2a) via a common metallation strategy, in which the corresponding free-base porphyrins bearing different peripheral substituents were reacted with zinc (II) salts under controlled conditions to afford the Zn^{2+} inserted macrocycles in good yields. All three compounds retained the characteristic planar porphyrinic core with a centrally coordinated Zn^{2+} ion, endowing them with intense Soret and Q-band absorptions, high photostability, and well-defined excited-state properties.[10]

Metalloporphyrins are particularly attractive optical sensing platforms owing to their strong visible absorption, tunable fluorescence, long-lived excited states, and the presence of a Lewis acidic metal center capable of axial coordination with a wide range of biologically relevant analytes.[11] Importantly, peripheral structural variation plays a decisive role in regulating solubility, steric environment, and supramolecular aggregation behavior in aqueous media, which in turn governs sensing performance. In the present system, the introduction of long alkyl chains (compound 2) enhanced hydrophobic interactions. It promoted strong aggregation, whereas bulky tert-butyl substituents (compound 3) sterically hindered close π–π stacking but altered excited-state relaxation pathways. Compound 1, lacking excessive steric bulk or hydrophobic shielding, achieved an optimal balance between aggregation and accessibility of the Zn^{2+} center, expecting to show superior optical response toward biological targets. These observations underscore that rational structural modulation of metalloporphyrin provides an effective strategy to tune aggregation-driven photophysics and optimize biosensing performance, offering valuable design principles for the development of next-generation optical sensors.

View Article Online
DOI: 10.1039/D6SD00054A

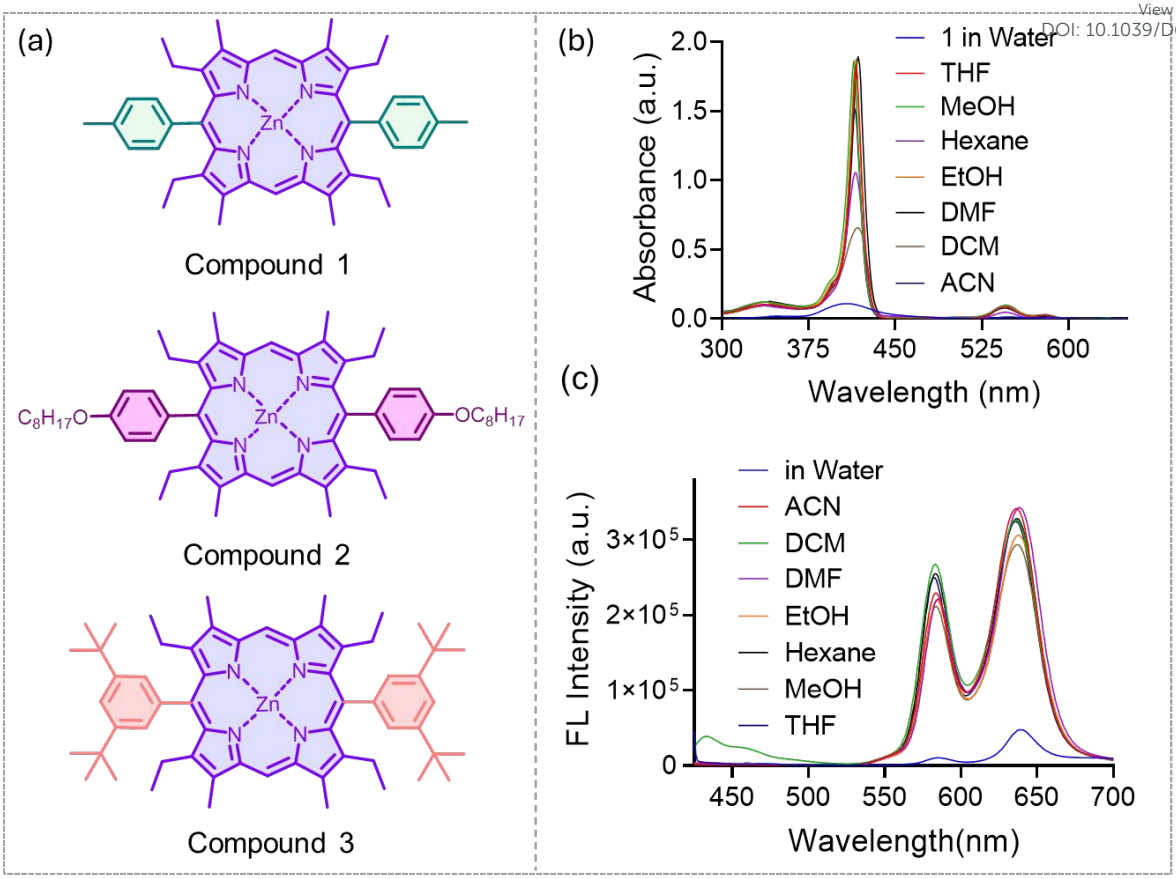

Figure 2. (a) Chemical structures of compounds (1-3) involved in the present study. (b) UV-visible spectra of compound 1 (10 μM) in different organic solvents and water (pH 7.4) medium. (c) Fluorescence spectra of compound 1 (10 μM, λex = 412 nm) in different organic solvents and water (pH 7.4) medium.

Solvatochromic Response and Photophysical Properties: The UV-visible spectra of compound 1 showed characteristic porphyrinic absorption bands in organic solvents, dominated by an intense Soret (B) band in the ~412-420 nm region and two weaker Q-bands in the ~540–590 nm range, (Figure 2b) originating from π–π* transitions of the macrocyclic conjugated system perturbed by Zn^{2+} coordination.[12] Across organic solvents of varying polarity, the Soret band showed only marginal solvatochromic shifts (typically ≤10 nm) and retained high molar absorptivity (ε on the order of 10^5 M^{-1} cm^{-1}), indicating that the ground and excited singlet states possessed comparable dipole moments and that nonspecific dielectric stabilization rather than strong solute-solvent interactions governed the spectral response. A minor redistribution of Q-band intensities and slight red shifts in more polar solvents can be attributed to a weak solvent-induced symmetry perturbation and subtle changes in vibronic coupling within the planar Zn–porphyrin framework. In contrast, in an aqueous medium, the absorption spectra display pronounced broadening, strong hypochromicity, and small but noticeable shifts of the Soret band, reflecting the disruption of the monomeric electronic structure due to

View Article Online
DOI: 10.1039/D6SD00054A

strong intermolecular interactions.[13] These features are consistent with exciton coupling in aggregated species, where π–π stacking of the hydrophobic porphyrin cores in water leads to partially slipped aggregates, effectively lowering the apparent oscillator strength and modifying the allowed electronic transitions.

On the other hand, compound 1 exhibited well-resolved dual emission bands in organic solvents, at 582 and 635 nm, corresponding to the 0-0 and 0-1 transitions, respectively. (Figure 2c) These kinds of relatively small Stokes shifts (<15 nm) with moderate fluorescence quantum yields (Φ_F ~ 0.03–0.06) indicated the presence of rigid, planar chromophore that could undergo minimal excited-state geometric relaxation.[14, 15] A slight red-shift and modest intensity modulation of the emission with increasing solvent polarity could be attributed by weak stabilization of the lowest singlet excited state (S_1) relative to the ground state (S_0), without introducing significant non-radiative decay pathways. In sharp contrast, fluorescence in aqueous medium was found to be severely quenched, accompanied by loss of vibronic structure, which can be ascribed to aggregation-induced quenching (ACQ). The poor solvation of compound 1 in water might promote hydrophobic collapse and strong π–π interactions, leading to exciton delocalization over aggregated porphyrin units and the formation of optically forbidden low-energy excited states. Consequently, radiative decay was suppressed in favor of non-radiative pathways such as internal conversion and intersystem crossing, resulting in dramatically reduced fluorescence lifetimes and quantum yields (Φ_F < 0.01).

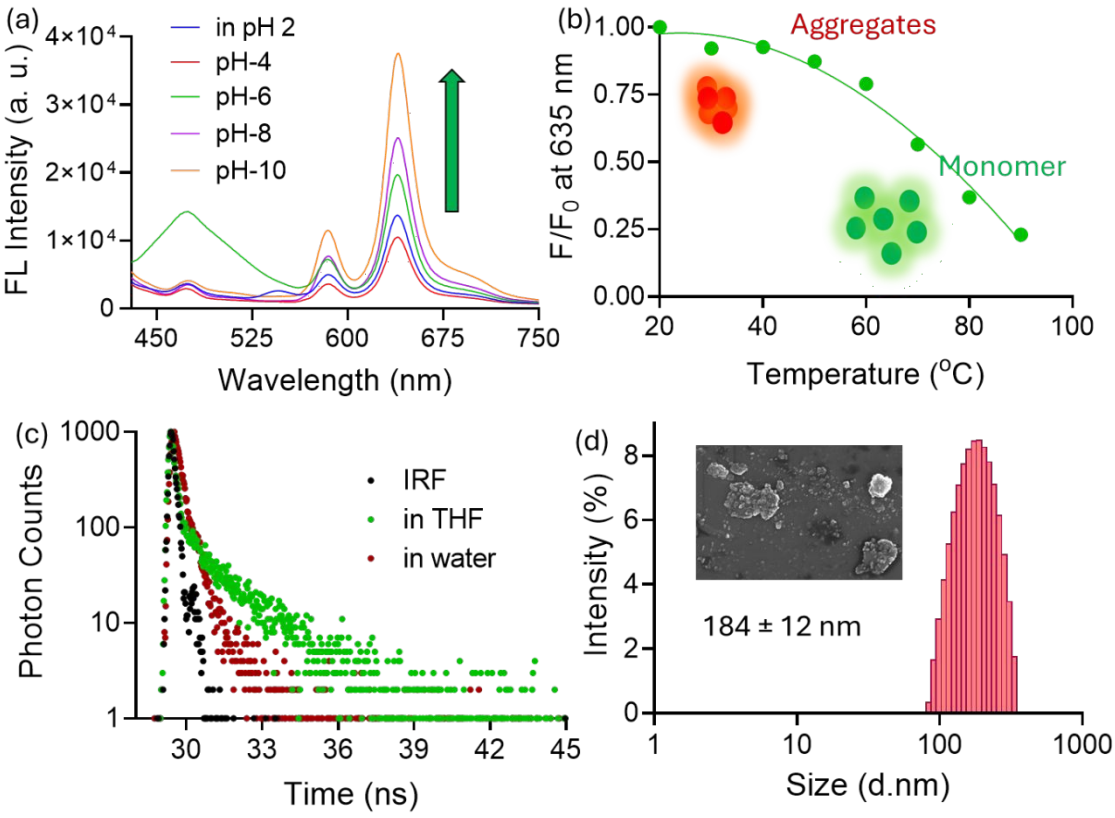

View Article Online
DOI: 10.1039/D6SD00054A

Figure 3. (a) Fluorescence spectra of compound 1 (10 μM, λex = 412 nm) at different pH conditions in buffered media. (b) Changes in fluorescence intensity of compound 1 (10 μM, λex = 412 nm) at 635 nm at different temperature in aqueous medium (pH 7.4). (c) Fluorescence lifetime of compound 1 (10 μM, λex = 412 nm) at 635 nm in THF and aqueous medium (pH 7.4). (d) DLS and FESEM image (Inset) of compound 1 in aqueous medium (pH 7.4).

Self-Assembly Behavior in Aqueous Medium: Time-resolved fluorescence studies revealed solvent-dependent changes in the excited-state lifetime of compound 1. In THF, the decay profile was found to be predominantly monoexponential in nature with an average 1.7 ns. (Figure 3c) Such a relatively long lifetime with a narrow lifetime distribution confirmed that compound 1 mostly existed in a well-solvated monomeric state in THF. In sharp contrast, the fluorescence decay in water showed a strongly multiexponential behavior with a markedly reduced average lifetime, dominated by fast decay components in the sub-nanosecond regime (1.2 ns). This substantial shortening of lifetime could directly be correlated with aggregation-induced excitonic coupling between closely packed porphyrin units.[16, 17] The emergence of a fast decay component indicates enhanced non-radiative deactivation in the aggregated state, arising from exciton delocalization and electronic coupling. DLS measurements in aqueous medium reveal nanoscale aggregates with an average hydrodynamic size of 176 ± 15 nm (Figure 3d), significantly larger than the monomeric dimensions. FESEM images further show irregular clustered morphologies (inset, Figure 3d), supporting the formation of supramolecular assemblies. These results collectively confirm the intrinsic tendency of compound 1 to self-associate in aqueous medium.

The fluorescence spectra of compound 1 recorded as a function of pH (2-10) in buffered aqueous medium exhibited a pronounced pH-responsive emission behavior, directly reflecting changes in its aggregation properties. (Figure 3a) With a gradual increase in pH, a systematic enhancement of fluorescence intensity was observed, accompanied by partial recovery of the characteristic dual emission bands of Zn–porphyrins. This fluorescence “turn-on” response was attributed to the progressive disruption of supramolecular aggregates, plausibly arising from the coordination of hydroxide ions to the Zn^{2+} center.[18] Such coordination was expected to sterically hinder close π–π stacking between porphyrin macrocycles and simultaneously improve hydration of the chromophoric core, thereby weakening intermolecular interactions responsible for aggregation-induced quenching. As a result, the excited state became increasingly localized on individual porphyrin units, restoring radiative decay pathways and enhancing the effective fluorescence quantum yield. The observed pH-dependent fluorescence modulation thus provided clear photophysical evidence that aggregation in water was reversible and stimulus-responsive, with proton activity acting as a key external parameter

View Article Online
DOI: 10.1039/D6SD00054A

governing the equilibrium between aggregated, non-emissive species and emissive monomer-like Zn–porphyrin states. Further, the variable temperature studies showed a monotonic decrease in fluorescence intensity with increasing temperature, accompanied by a systematic deviation from linearity. (Figure 3b) At lower temperatures, reduced thermal motion could stabilize supramolecular assemblies through favorable enthalpic contributions from π–π stacking and hydrophobic interactions.[19] As the temperature increased, the enhanced molecular motion and entropic contributions progressively weakened these noncovalent interactions, shifting the equilibrium toward smaller aggregates or partially dissociated species. The nonlinear temperature dependence of the aggregation signal suggested cooperative disassembly rather than a simple two-state process, consistent with the presence of polydisperse aggregate populations in solution.

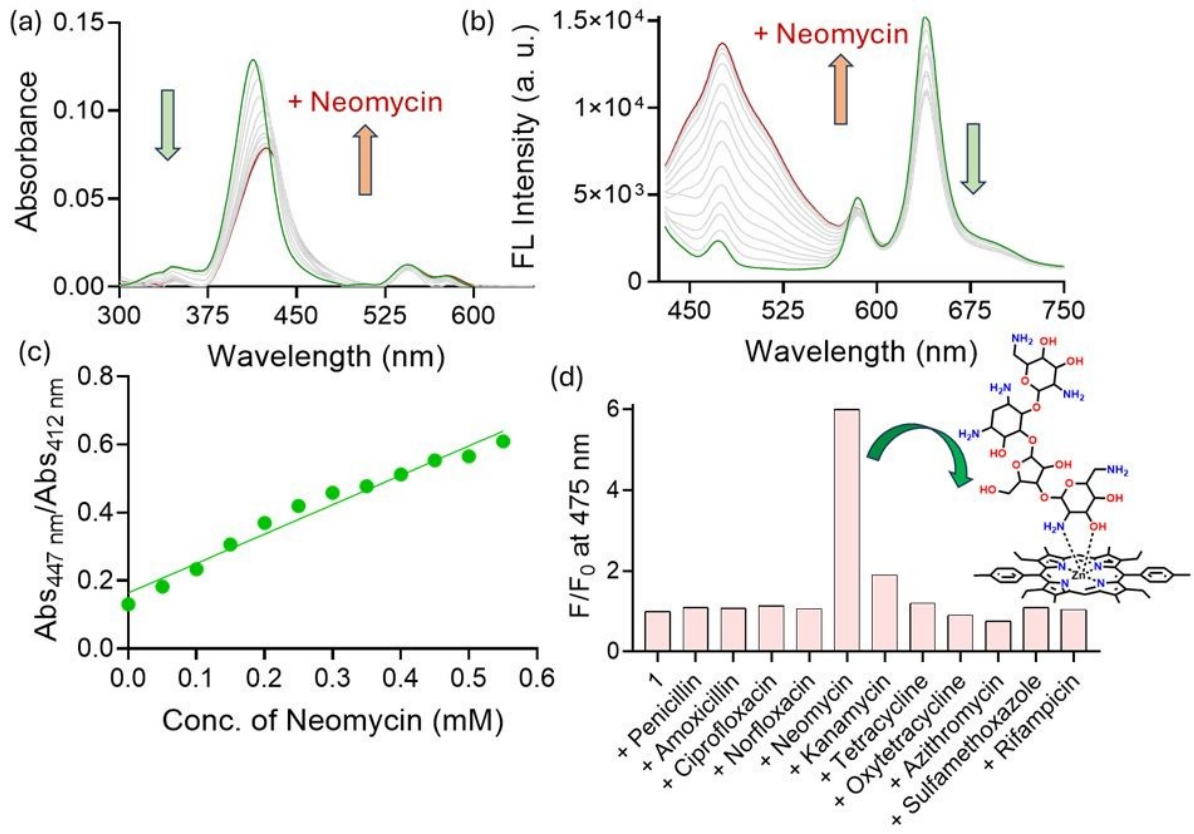

Figure 4. (a) UV-visible titration (b) Fluorescence titration of compound 1 (10 μM) with neomycin (0 – 0.65 mM) in aqueous medium (pH 7.4). (c) Changes in absorbance of compound 1 (10 μM) with neomycin (0 – 0.65 mM) in aqueous medium (pH 7.4). (d) Changes in fluorescence intensity of compound 1 (10 μM, λex = 412 nm) at 475 nm upon addition of different antibiotics (0.7 mM) in aqueous medium (pH 7.4).

Spectroscopic Response towards Aminoglycoside Glycosides: After realizing the photophysical properties as well as aggregation behavior of compound 1 in the aqueous medium, we proceeded to instigate the interaction of compound 1 with a series of antibiotics

View Article Online
DOI: 10.1039/D6SD00054A

in aqueous medium at physiological pH (7.4). A distinct and selective color change from orange to red was observed exclusively in the presence of aminoglycoside antibiotics, with neomycin producing the most pronounced response. Correspondingly, UV–visible absorption titration of compound 1 with neomycin resulted in a gradual and concentration-dependent red-shift of the Soret band from 412 to 425 nm, accompanied by a ~1.6-fold hypochromic effect and substantial spectral broadening. (Figure 4a) In contrast, the Q-band region exhibited comparatively minor changes, indicating that the interaction predominantly perturbed the higher-energy π–π* transitions of the porphyrin macrocycle.[20] These spectral changes indicate perturbation of the porphyrin electronic environment due to neomycin-induced modulation of supramolecular organization. Considering the Lewis acidic Zn^{2+} center and the polyaminated nature of neomycin, the absorption changes are attributed to axial coordination assisted by electrostatic and hydrogen-bonding interactions, leading to disruption of π–π stacked aggregates and altered excitonic coupling. The ratiometric absorption response (Abs_{447}/Abs_{412}) shows a clear linear increase with neomycin concentration (Figure 4c), indicating controlled interaction involving aggregate reorganization.

Consistent with the absorption studies, fluorescence titration of compound 1 with neomycin under identical conditions revealed pronounced ratiometric changes in the emission profile. Upon gradual addition of neomycin, the characteristic Zn–porphyrin emission bands at 582 and 635 nm were progressively quenched, while a new and well-defined emission band emerged at lower wavelength (~475 nm). (Figure 4b) The simultaneous quenching of the native porphyrin emission and appearance of a new emissive feature indicated the formation of a distinct excited-state species associated with neomycin interaction. This behavior was attributed to neomycin-triggered reorganization of the aggregated porphyrin assemblies, wherein coordination of amino functionalities to the Zn^{2+} center and strong electrostatic association collectively disrupted exciton delocalization within the aggregates. As a consequence, new radiative decay pathways became accessible, giving rise to the observed ratiometric fluorescence response. The absence of comparable spectral changes in the presence of non-aminated antibiotics further supported the critical role of amino groups in mediating this interaction. The fluorescence titration studies also indicated that the present system could detect neomycin as low as 2.8 μM in buffered medium. Further, the selectivity of compound 1 toward different classes of antibiotics was evaluated by monitoring the normalized fluorescence response (F/F_0) at 475 nm in aqueous medium (pH 7.4). The antibiotics tested included structurally diverse classes such as β-lactams (penicillin, amoxicillin), fluoroquinolones (ciprofloxacin, norfloxacin), aminoglycosides (neomycin, kanamycin), tetracyclines (tetracycline, oxytetracycline), macrolides (azithromycin), sulfonamides (sulfamethoxazole), and rifamycins (rifampicin). Among these, aminoglycosides

View Article Online
DOI: 10.1039/D6SD00054A

showed a pronounced fluorescence enhancement, with neomycin exhibiting the highest response (~6-fold), followed by a comparatively lower response for kanamycin (~3-fold). In contrast, other antibiotic classes produced minimal changes (F/F_0 ~1–1.5), remaining close to baseline. These results indicate a preferential and discriminative response toward aminoglycosides, with maximum sensitivity toward neomycin, rather than absolute selectivity. (Figure 4d) To further evaluate potential interference from structurally related aminoglycosides, fluorescence titration experiments of compound 1 were performed with kanamycin over a concentration range of 0-0.65 mM under identical experimental conditions. Upon gradual addition of kanamycin, a discernible increase in fluorescence intensity at 475 nm was observed, confirming that compound 1 responded to aminoglycosides in general. However, even at equivalent concentrations, the magnitude of fluorescence enhancement induced by kanamycin was ~3-fold weaker than that observed in the presence of neomycin. (Figure 5a) The difference was attributed to structural variations between the two aminoglycosides, particularly the higher density and more favorable spatial arrangement of amino functionalities in neomycin, which enabled stronger multivalent electrostatic interactions and more effective axial coordination to the Zn^{2+} center. These results demonstrated that compound 1 not only discriminated aminoglycosides from other antibiotic classes but also exhibited preferential sensitivity toward neomycin over closely related analogues.

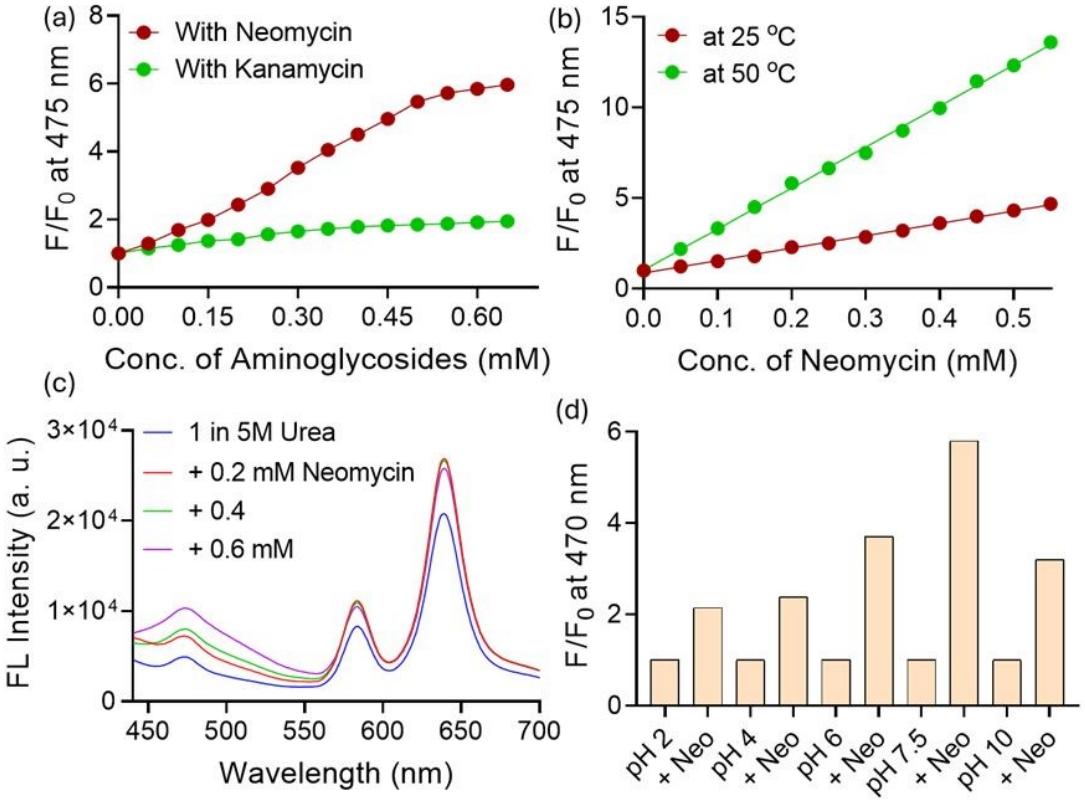

View Article Online
DOI: 10.1039/D6SD00054A

Figure 5. (a) Changes in fluorescence intensity of compound 1 (10 μM, λex = 412 nm) at 475 nm upon addition of neomycin and kanamycin (0-0.65 mM) in aqueous medium (pH 7.4). (b) Changes in fluorescence intensity of compound 1 (10 μM, λex = 412 nm) at 475 nm upon addition of neomycin (0-0.6 mM) at two different temperatures in aqueous medium (pH 7.4). (c) Fluorescence titration of compound 1 (10 μM, λex = 412 nm) with neomycin (0 – 0.6 mM) in presence of urea (5 M) in buffered media (pH 7.4). (d) Changes in fluorescence intensity of compound 1 (10 μM, λex = 412 nm) at 475 nm upon addition of neomycin (0.65 mM) at different pH conditions in buffer medium.

Effects of Microenvironment on Sensing Efficacy: To unveil the molecular insight of the interaction, we performed a series of spectroscopic experiments with neomycin. The temperature-dependent fluorescence response of compound 1 toward neomycin was examined by performing fluorescence titrations at 25 °C and 50 °C, where a clear enhancement in sensitivity was observed at elevated temperature. At both temperatures, the normalized fluorescence intensity (F/F_0) at 475 nm increased monotonically with neomycin concentration. However, the response was substantially high at 50 °C (~13.7-fold). (Figure 5b) This behavior suggested that neomycin-induced modulation of the Zn–porphyrin aggregates was thermodynamically favored at higher temperatures.[21, 22] The enhanced response was attributed to partial thermal destabilization of porphyrin aggregates, wherein increased thermal energy weakened π–π stacking and hydrophobic interactions that stabilize the aggregated state, thereby increasing accessibility of the Zn^{2+} centers to neomycin. From a thermodynamic perspective, the interaction appeared to be driven by a favorable entropy change ($\Delta S > 0$), arising from aggregate disassembly, increased conformational freedom of the porphyrin units, and release of structured water molecules from the hydrophobic porphyrin surface upon neomycin binding.[23] Although axial coordination of amino functionalities to the Zn^{2+} center likely contributed an enthalpic component ($\Delta H < 0$) through metal-ligand interactions and electrostatic stabilization, the observed temperature dependence indicated that the overall sensing process was predominantly entropy-driven.

Along with temperature, the pH-dependent fluorescence response of compound 1 toward neomycin was systematically evaluated by comparing the normalized emission intensity (F/F_0) at 470 nm both with and without neomycin across a broad pH range (2–10). At all investigated pH values, addition of neomycin resulted in enhancement in fluorescence intensity, with the magnitude of the response increasing progressively from acidic pH 2 to mildly acidic pH 4, further intensifying at pH 6, and reaching a maximum at physiological pH 7.4. Notably, at pH 10, the fluorescence response toward neomycin decreased significantly compared to that at pH 7.4. (Figure 5d) This nonmonotonic pH dependence was attributed to the combined

View Article Online
DOI: 10.1039/D6SD00054A

influence of porphyrin aggregation behavior, neomycin protonation state, and Zn^{2+} coordination chemistry.[24] At low pH, extensive protonation of amino functional groups pf neomycin reduced effective electrostatic and coordination interactions, limiting analyte-induced aggregate reorganization. [25] As the pH increased toward neutrality, optimal protonation of the aminoglycoside enabled strong multivalent electrostatic interactions and plausible axial coordination of amino groups to the Zn^{2+} center, resulting in efficient disruption of π-π stacked aggregates and enhanced formation of the interaction-induced emissive species. At highly basic pH, however, competitive coordination of hydroxide ions to the Zn^{2+} center and partial deprotonation of neomycin diminished its binding affinity, while excessive destabilization of aggregates reduced the cooperative reorganization process, collectively leading to attenuation of the fluorescence response.[26]

Mechanistic Insight into Neomycin Binding Isotherm: Also, the influence of competitive hydrogen-bonding and denaturing conditions on the fluorescence response of compound 1 toward neomycin was examined by performing fluorescence measurements in the presence of excess urea (5 M). Under these conditions, the fluorescence enhancement induced by neomycin was found to be significantly suppressed compared to that observed in urea-free aqueous medium. (Figure 5c) This attenuation of response was attributed to the strong hydrogen-bonding ability of urea, which effectively competed with neomycin for noncovalent interactions with the porphyrin framework and disrupted the hydration shell surrounding the aggregates.[27, 28] In addition, urea is known to weaken hydrophobic interactions and π–π stacking by altering solvent structure, thereby destabilizing the aggregation equilibrium that is central to the sensing mechanism of compound 1. The presence of excess urea therefore reduced the efficiency of neomycin-induced aggregate reorganization and weakened coordination-assisted binding at the Zn^{2+} center, leading to diminished formation of the interaction-induced emissive species.

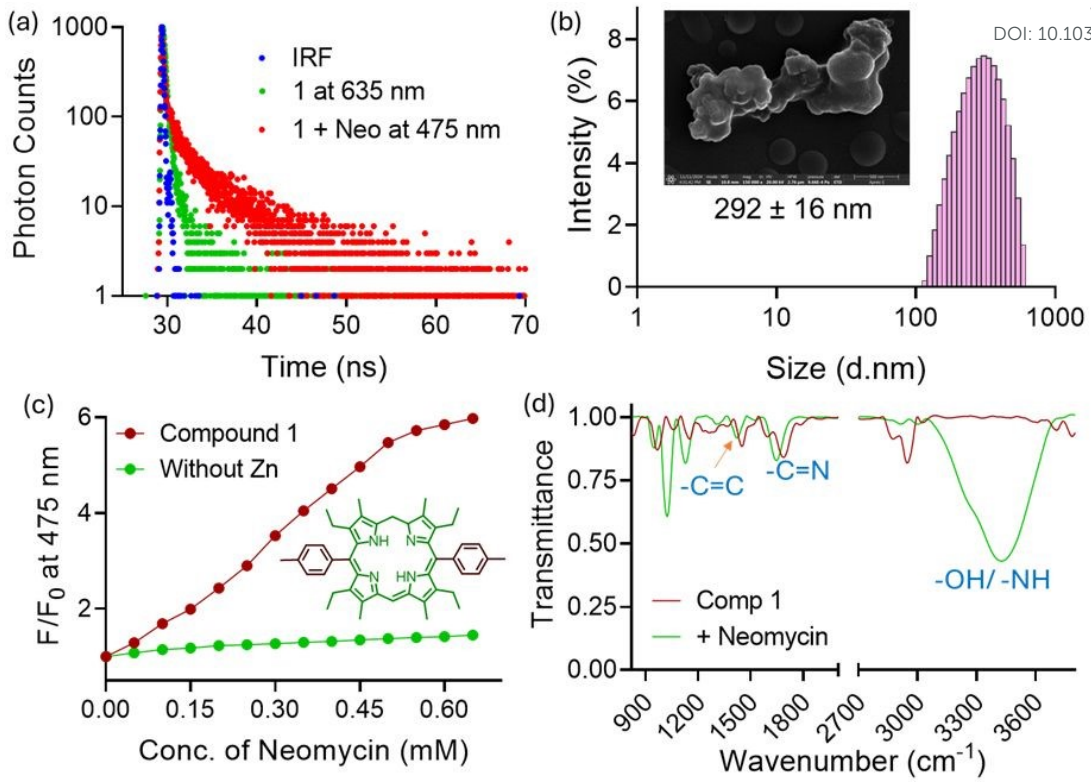

Figure 6. (a) Fluorescence Lifetime spectra of compound 1 (10 μM, λex = 412 nm) upon addition of neomycin (0.65 mM) in aqueous medium (pH 7.4). (b) DLS and FESEM image (Inset) of 1 with neomycin (0.6 mM) in aqueous medium (pH 7.4). (c) Changes in fluorescence intensity of 1 the its corresponding demetallated precursor (10 μM, λex = 412 nm) upon addition of neomycin (0 - 0.65 mM) in aqueous medium (pH 7.4) (d) FT-IR spectra of 1 with neomycin.

Time-resolved fluorescence measurements of compound 1 in the presence of neomycin revealed a marked alteration in excited-state decay dynamics compared to the aggregated state of compound 1 alone in aqueous medium. (1.2 ns to 1.8 ns) (Figure 6a) The fluorescence decay profiles became distinctly multiexponential, with the appearance of longer-lived decay components relative to the probe alone, indicating suppression of ultrafast non-radiative deactivation pathways associated with aggregation-induced quenching. This lifetime prolongation directly correlated with the emergence of the interaction-induced emissive state observed at ~475 nm, suggesting partial localization of the excited state following neomycin binding. Dynamic light scattering (DLS) measurements provided complementary structural evidence for neomycin-induced changes in aggregation behavior. In the presence of neomycin, the hydrodynamic size distribution shifted toward larger and more polydisperse assemblies compared to compound 1 alone, (Figure 6b), indicating restructuring and reorganization of pre-existing porphyrin aggregates rather than complete disassembly into monomeric species. This increase in aggregate size was attributed to multivalent electrostatic

View Article Online
DOI: 10.1039/D6SD00054A

interactions and coordination-assisted cross-linking between the polycationic aminoglycoside and multiple porphyrin units, resulting in the formation of reorganized supramolecular architectures. Consistent with the DLS data, FESEM imaging revealed irregular, clustered morphologies with interconnected, fused aggregate domains, markedly different from the relatively compact aggregates observed for compound 1 in the absence of neomycin. These morphological features confirmed that neomycin acted as a supramolecular modulator, promoting aggregate fusion and reassembly through cooperative electrostatic, hydrogen-bonding, and axial coordination interactions with the Zn^{2+} centers. [29]

To elucidate the role of the metal center in antibiotic recognition, a control experiment was performed using the corresponding free-base porphyrin lacking the Zn^{2+} ion under identical experimental conditions. In sharp contrast to compound 1, the metal-free porphyrin exhibited only negligible changes in fluorescence intensity upon addition of neomycin over the same concentration range. (Figure 6c) The drastically reduced response of the free-base porphyrin was attributed to the absence of an accessible Lewis acidic coordination site, which precluded axial binding of the amino functionalities of neomycin.[30] Without Zn^{2+}-mediated coordination, the interaction was limited to weak, nonspecific electrostatic or hydrophobic contacts that were inadequate to perturb the aggregation equilibrium or excitonic coupling within the porphyrin assemblies. Consequently, neomycin failed to induce significant aggregate reorganization or generate the interaction-induced emissive species observed at 475 nm for compound 1. These results unambiguously established the central Zn^{2+} ion as a critical structural and functional element for neomycin recognition, confirming that coordination-assisted aggregation modulation was the dominant mechanism governing the selective sensing behavior of compound 1.

FT-IR spectra of compound 1 recorded before and after exposure to neomycin revealed clear vibrational changes indicative of specific intermolecular interactions. The spectrum of compound 1 alone exhibited characteristic porphyrinic vibrational features, including bands associated with macrocyclic C=C and C–N stretching modes in the fingerprint region, along with relatively weak and narrow bands in the higher wavenumber region. Upon addition of neomycin, several notable spectral modifications were observed, including broadening and intensity enhancement in the 3200-3600 cm^{-1} region corresponding to O–H and N–H stretching vibrations, (Figure 6d) consistent with increased hydrogen bonding and altered solvation around the porphyrin framework. In addition, discernible changes in band intensity and position were detected in the 1500-1700 cm^{-1} region, suggesting perturbation of the porphyrin electronic environment and possible involvement of amino functionalities of neomycin in binding interactions. Subtle shifts in bands associated with porphyrin core vibrations further indicated modification of the local coordination environment. These spectral

View Article Online
DOI: 10.1039/D6SD00054A

changes were attributed to the formation of coordination-assisted and hydrogen-bond-mediated interactions between neomycin and compound 1. The emergence and broadening of N–H/O–H stretching features supported strong hydrogen bonding and electrostatic association between the polyaminated aminoglycoside and the porphyrin assembly. Moreover, the perturbation of porphyrin skeletal vibrations was consistent with plausible axial coordination of amino groups to the Zn^{2+} center, leading to redistribution of electron density within the macrocycle. [31]

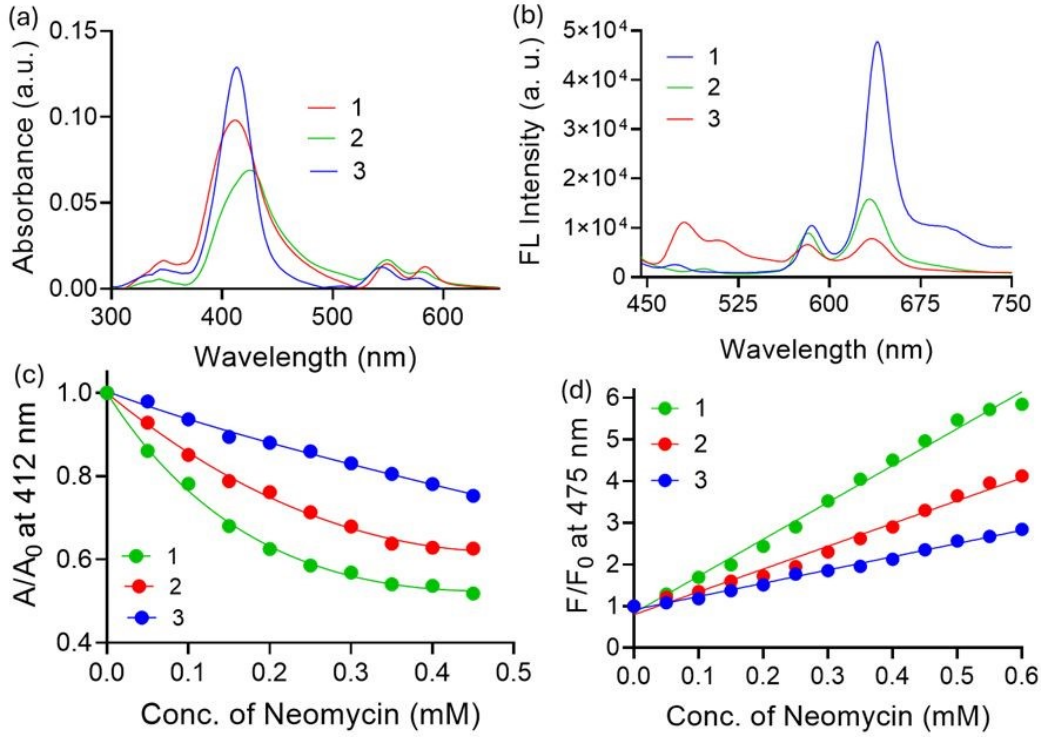

Figure 7. (a) UV-visible spectra of compounds 1-3 (10 μM) in aqueous medium (pH 7.4). (b) Fluorescence spectra of 1-3 (10 μM, λex = 412 nm) in aqueous medium (pH 7.4) (c) Changes in absorbance of compounds 1-3 (10 μM) upon addition of neomycin (0 - 0.45 mM) in aqueous medium (pH 7.4) (d) Changes in fluorescence intensity of 1-3 (10 μM, λex = 412 nm) at 475 nm upon addition of neomycin (0 - 0.60 mM) in aqueous medium (pH 7.4)

we have now performed XPS analysis of compound 1 before and after interaction with neomycin. The Zn 2p spectrum of compound 1 displayed the characteristic Zn $2p_{3/2}$ and Zn $2p_{1/2}$ signals centered around 1021 and 1044 eV, respectively. Upon interaction with neomycin, discernible changes in the Zn 2p binding environment were observed, indicating perturbation of the electronic density around the Zn^{2+} center. These spectral changes are consistent with axial coordination of the amino functionalities of neomycin to the Zn^{2+} center of the porphyrin framework. (Figure S1)

View Article Online
DOI: 10.1039/D6SD00054A

Effects of Terminal Functional Groups on Aminoglycoside Sensing: The UV–visible absorption spectra of Zn–porphyrin complexes 1–3 recorded in aqueous medium at pH 7.4 exhibited pronounced differences, reflecting their distinct aggregation propensities governed by peripheral substituents. (Figure 7a) Compound 1 displayed moderate broadening and partial hypochromicity of the Soret band, indicative of aggregate formation arising from hydrophobic and π–π interactions in water. In contrast, compound 2, bearing long alkyl chains at the terminal positions, showed the most pronounced spectral perturbations, including significant Soret band broadening and hypochromicity along with reduced spectral definition.[11, 32] These features were consistent with enhanced hydrophobic interactions promoted by the flexible alkyl chains, which facilitated stronger π–π stacking and formation of larger supramolecular aggregates. Conversely, compound 3, functionalized with bulky tert-butyl groups, exhibited relatively sharp and intense Soret and Q bands with minimal broadening, suggesting poor aggregation in aqueous medium. The steric bulk of the tert-butyl substituents effectively hindered close face-to-face stacking of the porphyrin macrocycles, thereby suppressing excitonic coupling. Collectively, the UV–visible data established that aggregation strength followed the order 2 > 1 > 3, directly correlating with the hydrophobicity and steric profile of the peripheral substituents. (Figure S3)

The fluorescence profiles reveal a nuanced aggregation–emission relationship. At ~638 nm, the intensity follows the order 1 > 2 > 3 (Figure 7b). The weak emission of compound 3 indicates that steric inhibition of π–π stacking alone does not enhance red emission; instead, bulky tert-butyl groups disrupt excited-state relaxation and suppress population of the S_1 state responsible for porphyrinic emission.[33] Notably, compound 3 exhibited an additional high-energy emission band at ~475 nm, absent in compounds 1 and 2, attributed to a conformation-induced emissive state arising from restricted relaxation and altered excitonic coupling. In contrast, compound 1 maintains an optimal balance between aggregation and excited-state localization, showing the highest emission at 638 nm, while compound 2 undergoes aggregation-induced quenching due to strong exciton delocalization. The emission behavior of compound 3 closely resembles that of compound 1 upon neomycin addition, suggesting that steric congestion in 3 mimics analyte-induced aggregate reorganization, promoting emission from a higher-energy state.

The response of compounds 1–3 toward neomycin (Figure 7c,d) shows a clear dependence on peripheral structure. Compound 1 exhibits the strongest response, followed by 2, while 3 shows minimal change. This trend highlights the importance of balancing aggregation and Zn^{2+} accessibility. In compound 2, strong hydrophobic aggregation limits access to the Zn^{2+} center, reducing sensing efficiency, whereas in compound 3, steric hindrance restricts both aggregation and analyte interaction. Thus, efficient sensing arises from an optimal interplay

View Article Online
DOI: 10.1039/D6SD00054A

between aggregation, steric accessibility, and coordination capability, achieved in compound 1.

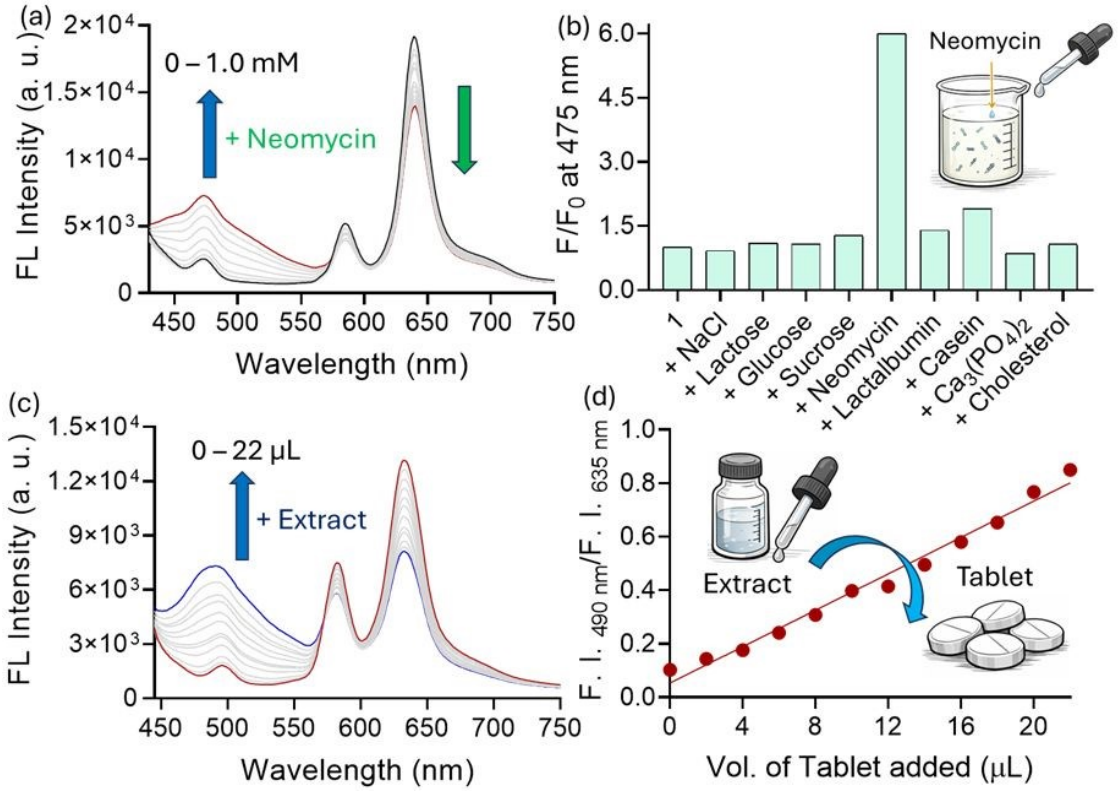

Figure 8. (a) Fluorescence titration of 1 (10 µM, λex = 412 nm) with neomycin (0 – 1 mM) in diluted milk solution, 20 % (v/v) in pH 7.4 buffer. (b) Changes in fluorescence intensity of 1 (10 µM, λex = 412 nm) in presence of various other milk components in aqueous medium (pH 7.4) (c) Fluorescence titration of 1 (10 µM, λex = 412 nm) with neomycin tablet extract (0 – 20 µL) in aqueous medium (pH 7.4) (d) Ratiometric changes in fluorescence intensity of 1 (10 µM, λex = 412 nm) upon addition of tablet extract (0 – 20 µL) in aqueous medium (pH 7.4)

Screening of Food and Pharmaceutical Formulations for Neomycin: Considering the potential toxicity and widespread use of neomycin, and the associated risks of antibiotic residues in food products, the practical applicability of compound 1 was evaluated by estimating neomycin content in commercially available milk samples. (Figure 1) The presence of neomycin residues in milk is of particular concern due to their possible adverse effects on human health and contribution to antimicrobial resistance, necessitating reliable and rapid monitoring strategies.[34] Milk samples were initially diluted to 20 % (v/v) with phosphate buffer (pH 7.4) to minimize matrix effects and then spiked with known concentrations of neomycin in the range of 0-0.1 mM. Upon addition of neomycin, the fluorescence spectra of compound 1 displayed a clear and concentration-dependent enhancement of the interaction-induced emission band centered at ~475 nm, accompanied by quenching of the native porphyrin emission. (Figure

View Article Online
DOI: 10.1039/D6SD00054A

8a) A good linear correlation between fluorescence intensity at 475 nm and neomycin concentration was obtained within the investigated range, confirming quantitative detection capability in the diluted milk matrix. (Figure S2a) The limit of detection under these conditions was estimated to be 0.75 μM, demonstrating sufficient sensitivity for practical analysis. A comparative analysis of previously reported neomycin detection methods in milk samples is provided in Table S1. To verify that the observed fluorescence response originated solely from neomycin, control experiments were conducted using individual milk components and unspiked milk samples, none of which produced any significant change in emission intensity. (Figure 8b) Recovery studies performed using spiked milk samples yielded satisfactory recovery values (98.7-104.2 %), confirming minimal interference from the sample matrix and validating the reliability of the sensing platform for real-world analysis.

The applicability of the system was further evaluated using a commercial tablet formulation. A tablet extract was prepared and incrementally added to an aqueous solution of compound 1 under identical conditions. A linear increase in fluorescence intensity at 475 nm was observed with increasing extract volume (Figure 8c, d), confirming a quantitative response in the presence of excipients. Control experiments with common additives showed negligible interference. (Figure S2b) The estimated neomycin content closely matched the labeled value, demonstrating the analytical reliability of the method.[35]

Chemically-modified Paper Strips for On-location Detection Purposes: For practical, on-site detection of neomycin, paper-based sensing platforms were fabricated by drop-casting a THF solution of compound 1 onto cellulose filter paper discs, followed by air drying under ambient conditions. The paper strips, as-prepared, exhibited faint red fluorescence under UV illumination in the absence of analyte, consistent with the aggregated and weakly emissive state of compound 1 immobilized on the solid support.[36, 37] Nevertheless, FESEM analysis confirmed uniform deposition of compound 1 along the cellulose fiber network, indicating successful immobilization without macroscopic phase separation. FT-IR spectra of the coated paper strips displayed characteristic vibrational bands corresponding to the porphyrin framework, including –C=C and –C=N– stretching modes, in addition to cellulose-derived features. (Figure 9a) The observed shift in the –OH stretching vibration of cellulose, together with changes in the fingerprint region, suggested strong interfacial hydrogen bonding between compound 1 and the hydroxyl-rich cellulose matrix.[38]

Before analyzing the analyte-induced response, the operational robustness of the paper strips was systematically evaluated. Time-dependent stability studies demonstrated negligible loss of fluorescence response over a period of 0–5 days under ambient storage conditions. Thermal stability tests showed that the neomycin-induced fluorescence response remained

View Article Online
DOI: 10.1039/D6SD00054A

essentially unchanged at 20 and 40 °C, with only a minor reduction observed at 40 °C. (Figure 9b) Furthermore, the sensing performance was largely unaffected by relative humidity variations of 20 and 80 %, confirming strong resistance to moisture-induced interference. Collectively, these results established that the probe-coated paper strips were mechanically robust, chemically stable, and environmentally resilient. Owing to their low cost, portability, ease of operation, and independence from controlled pH, temperature, or external power sources, this paper-based platform offers a practical and field-deployable approach for selective and concentration-dependent detection of neomycin in real-world settings.

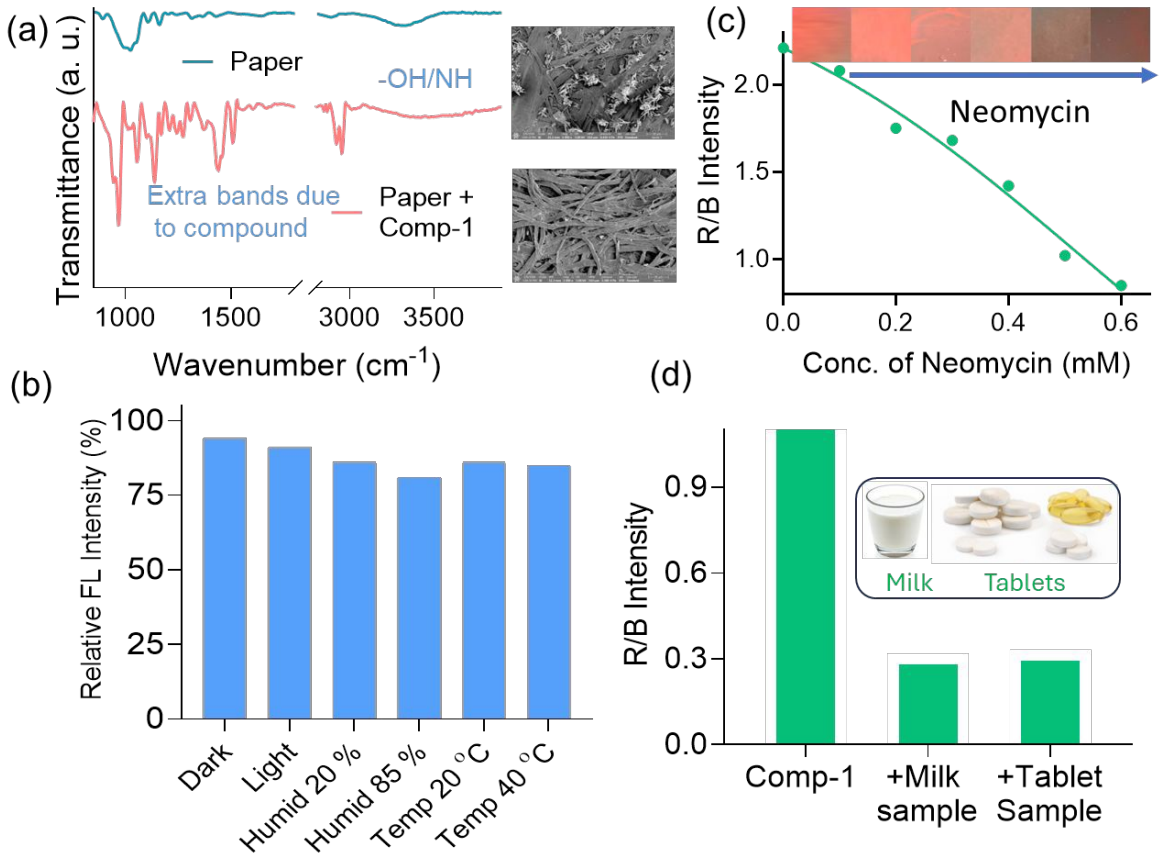

Figure 9. (a) FTIR spectra and SEM images confirming probe immobilization on paper (b) Stability of the fluorescent paper under varying light, humidity, and temperature conditions. (c) Decrease in R/B ratio of the paper strip with increasing neomycin concentration, indicating concentration-dependent fluorescence quenching (d) RGB-based ratiometric (R/B) response showing a marked decrease upon neomycin detection in real samples.

Upon exposure of the functionalized paper strips to aqueous neomycin solutions, a pronounced and concentration-dependent fluorescence response was observed under UV illumination. The initially red-orange emission of the paper strips gradually transformed into a very faint orange color fluorescence with increasing neomycin concentration (0 – 0.6 mM), enabling direct visual detection by the naked eye. This behavior was attributed to neomycin-

View Article Online
DOI: 10.1039/D6SD00054A

triggered reorganization of aggregated Zn–porphyrin assemblies on the paper surface, driven by multivalent electrostatic interactions and plausible axial coordination of amino functionalities to the Zn^{2+} center. (Figure 10) The concentration-dependent evolution of emission color from faint red-orange to faint orange provided a reliable optical signature for neomycin detection. Furthermore, we evaluated the ratiometric red-to-blue (R/B) fluorescence response of the dye-coated paper before and after exposure to neomycin. (Figure 9c and d) For Compound 1, the addition of neomycin led to a pronounced decrease in the R/B ratio, reflecting effective fluorescence quenching arising from strong supramolecular interactions between the aminoglycoside and the probe. In real-sample matrices, including milk and tablet extracts, a similar reduction in R/B values was observed, confirming that the sensing response is retained despite matrix complexity.[39, 40]

Overall, this RGB-based ratiometric approach demonstrates the successful integration of neomycin-responsive fluorescent probes into paper-based platforms, offering high visual contrast, robustness under practical conditions, and reliable quantification using smartphone imaging. The simplicity of the R/B readout enables rapid, decentralized, and cost-effective detection of neomycin in real-world samples without the need for sophisticated instrumentation.

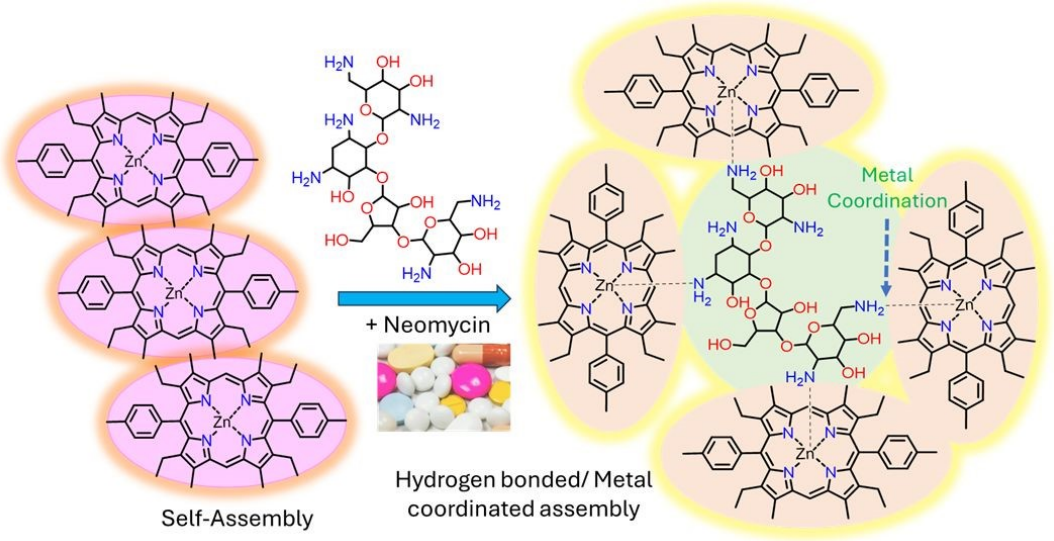

Figure 10. Schematic diagram shows the molecular-level interaction of compound 1 with Neomycin.

CONCLUSION

In summary, this work demonstrates a rationally designed Zn–porphyrin–based supramolecular sensing platform in which controlled aggregation and coordination chemistry were synergistically exploited for selective and sensitive detection of neomycin in aqueous media. Systematic structural modulation across three Zn–porphyrin derivatives revealed that

View Article Online
DOI: 10.1039/D6SD00054A

an optimal balance between aggregation propensity and accessibility of the Zn^{2+} center is critical for efficient sensing, with compound 1 outperforming its analogues bearing long alkyl chains or bulky tert-butyl substituents. Detailed photophysical investigations revealed that aggregation in water resulted in pronounced hypochromicity, fluorescence quenching, shortened excited-state lifetimes, and the formation of nanoscale assemblies. In contrast, neomycin binding induced a distinct reorganization of these aggregates. This interaction was manifested by a characteristic ratiometric fluorescence response involving quenching of the native porphyrinic emission (582/635 nm) and emergence of a new blue-shifted band at ~475 nm, enabling neomycin detection down to low micromolar levels. Mechanistic studies combining temperature, pH, urea competition, time-resolved fluorescence, DLS, FESEM, and FT-IR studies unequivocally established that neomycin recognition proceeds via coordination-assisted and electrostatic modulation of Zn–porphyrin aggregates, driven predominantly by favorable entropic contributions arising from aggregate reorganization and release of structured water. Importantly, the sensing concept was successfully translated to real-life applications, including quantitative analysis of neomycin in commercial milk and pharmaceutical formulations with excellent recovery (98.7-104.2 %) and accuracy, as well as to robust, low-cost paper strips enabling instrument-free, on-site visual detection through a clear red-to-blue fluorescence transition. The novelty of this study lies in leveraging aggregation not as a limitation but as an active, tunable transduction mechanism, offering a general design strategy for next-generation metalloporphyrin-based biosensors targeting clinically and environmentally relevant antibiotics.

CRediT authorship contribution statement

Nisha Chhetri, Satadru Jha, and Harshal V Barkale: Investigation, Data curation, Validation. Nilanjan Dey: Conceptualization, Formal analysis, Project administration, Resources, Software, Supervision, Visualization, Writing – original draft, Writing – review & editing.

Acknowledgments

N.D. thanks DST for the SYST grant [grant no. (SP/YO/2021/1632)] and the Ministry of Education (MOE), India, for the STARS grant (STARS2/2023-0300). N.D. and H.B. thank BITS Pilani, Hyderabad campus, for financial and technical support. The authors also thank the central analytical facilities at BITS Pilani, Hyderabad, for instrumental facilities.

Declaration of Competing Interest

The authors declare no competing financial interest.

Data availability

View Article Online
DOI: 10.1039/D6SD00054A

Data will be made available on request.

References:

1. Richardson, S. D.; Ternes, T. A. Water analysis: emerging contaminants and current issues. Anal. Chem. 2021, 94, 382–416.
2. Singh, P. K.; Kumar, U.; Kumar, I.; Dwivedi, A.; Singh, P.; Mishra, S.; Seth, C. S.; Sharma, R. K. Critical review on toxic contaminants in surface water ecosystem: sources, monitoring, and its impact on human health. Environ. Sci. Pollut. Res. 2024, 31, 56428–56462.
3. Sangster, T.; Major, H.; Plumb, R.; Wilson, A. J.; Wilson, I. D. A pragmatic and readily implemented quality control strategy for HPLC-MS and GC-MS-based metabonomic analysis. Analyst 2006, 131, 1075–1078.
4. Chirco, A.; Meacci, E.; Margheri, G. A tutorial review on surface plasmon resonance biosensors: applications in biomedicine. ACS Bio Med Chem Au 2025, 5, 922–946.
5. Scrimin, P.; Prins, L. J. Sensing through signal amplification. Chem. Soc. Rev. 2011, 40, 4488–4505.
6. Sajwan, R. K.; Hashmi, S.; Himanshu, J. K.; Kumari, A.; Solanki, P. R. Current advancement in nanomaterial-based emerging techniques for the determination of aminoglycosides antibiotics for antibiotic resistance surveillances. Mater. Adv. 2024, 5, 961–985.
7. Apley, M. D. Antimicrobial chemotherapy and antimicrobial resistance. Vet. Microbiol. 2022, 271, 771–802.
8. Le, T. A.; Hiba, T.; Chaudhari, D.; Preston, A. N.; Palowsky, Z. R.; Ahmadzadeh, S.; Shekoohi, S.; Cornett, E. M.; Kaye, A. D. Aminoglycoside-related nephrotoxicity and ototoxicity in clinical practice: a review of pathophysiological mechanism and treatment options. Adv. Ther. 2023, 40, 1357–1365.
9. Senge, M. O.; Sergeeva, N. N.; Hale, K. J. Classic highlights in porphyrin and porphyrinoid total synthesis and biosynthesis. Chem. Soc. Rev. 2021, 50, 4730–4789.
10. Lu, H.; Kobayashi, N. Optically active porphyrin and phthalocyanine systems. Chem. Rev. 2016, 116, 6184–6261.
11. Paolesse, R.; Nardis, S.; Monti, D.; Stefanelli, M.; Di Natale, C. Porphyrinoids for chemical sensor applications. Chem. Rev. 2017, 117, 2517–2583.

12. Schnetz, F.; Richeter, S.; Versace, D.-L. Porphyrin derivatives: promising perspectives in visible/IR light photopolymerization. Polym. Chem. 2025, 16, 1732–1791.

13. Kubat, P.; Lang, K.; Kral, V.; Anzenbacher, P. Preprogramming of porphyrin–nucleic acid assemblies via variation of the alkyl/aryl substituents of phosphonium tetratolylporphyrins. J. Phys. Chem. B 2002, 106, 6784–6792.

14. Ahmed, R.; Manna, A. K. Understanding high fluorescence quantum yield and simultaneous large Stokes shift in phenyl bridged donor–π–acceptor dyads with varied bridge lengths in polar solvents. J. Phys. Chem. A 2022, 126, 4221–4229.

15. Barkale, H. V.; Dey, N. Tailoring rhodamine probes: oxyethylene chains, conjugation, and end substituents in the quest for superior Hg^{2+} sensing. Asian J. Org. Chem. 2024, 13, e202300657.

16. Guan, J.; Shen, C.; Peng, J.; Zheng, J. What leads to aggregation-induced emission? J. Phys. Chem. Lett. 2021, 12, 4218–4226.

17. Barkale, H. V.; Maiti, B.; Dey, N. Planar vs. twisted pyrimidine derivatives: insights from molecular dynamics and predictive modelling for melamine detection in dairy products. Mater. Adv. 2025, 6, 6479–6492.

18. Shyamal, M.; Mazumdar, P.; Maity, S.; Samanta, S.; Sahoo, G. P.; Misra, A. Highly selective turn-on fluorogenic chemosensor for robust quantification of Zn(II) based on aggregation induced emission enhancement feature. ACS Sens. 2016, 1, 739–747.

19. Deng, J.-H.; Luo, J.; Mao, Y.-L.; Lai, S.; Gong, Y.-N.; Zhong, D.-C.; Lu, T.-B. π–π stacking interactions: non-negligible forces for stabilizing porous supramolecular frameworks. Sci. Adv. 2020, 6, eaax9976.

20. Mack, J. Expanded, contracted, and isomeric porphyrins: theoretical aspects. Chem. Rev. 2017, 117, 3444–3478.

21. Xi, H.; Davis, E.; Ranjan, N.; Xue, L.; Hyde-Volpe, D.; Arya, D. P. Thermodynamics of nucleic acid “shape readout” by an aminosugar. Biochemistry 2011, 50, 9088–9113.

22. Barkale, H. V.; Dey, N. Membrane-bound bisindolyl-based chromogenic probes: analysis of cyanogenic glycosides in agricultural crops for possible remediation. ACS Appl. Bio Mater. 2024, 8, 189–198.

23. Biswakarma, D.; Patra, S.; Dey, N. Pyrene-based amphiphilic fluorescent probe as a versatile optical platform for cardiac biomarker detection: from biological fluids to live cell imaging. Langmuir 2025, 41, 34565–34573.

View Article Online
DOI: 10.1039/D6SD00054A

24. Pattam, H. K.; Jadhav, A. B.; Cheran, A.; Marydasan, B.; Kumar, J. Zinc selective interactions of porphyrins aid conversion of nanoaggregates into luminescent microstructures: toward the development of a sensing platform. J. Phys. Chem. C 2023, 127, 17584–17591.

25. Chen, J.; Fan, Z.; Zhang, C.; Duan, H.; Fan, L.-J. Amphiphilic conjugated polyelectrolyte-based sensing system for visually observable detection of neomycin with high sensitivity. ACS Appl. Polym. Mater. 2021, 3, 2088–2097.

26. Maret, W.; Li, Y. Coordination dynamics of zinc in proteins. Chem. Rev. 2009, 109, 4682–4707.

27. Patra, S.; Dey, N. Unravelling the optical properties and self-assembly behavior of ciprofloxacin in ionic liquid environments: probing the role of cationic residues and counter anions. Dalton Trans. 2025, 54, 5502–5510.

28. Barkale, H. V.; Patra, S.; Dey, N. Integrating spectroscopy, molecular docking, and machine learning to decipher mycotoxin–protein-binding mechanisms. ACS Appl. Bio Mater. 2026.

29. Jadhav, R. W.; Kobaisi, M. A.; Jones, L. A.; Vinu, A.; Bhosale, S. V. The supramolecular self-assembly of aminoglycoside antibiotics and their applications. ChemistryOpen 2019, 8, 1154–1166.

30. Szyszko, B.; Białek, M. J.; Pacholska-Dudziak, E.; Latos-Grażyński, L. Flexible porphyrinoids. Chem. Rev. 2017, 117, 2839–2909.

31. Dar, U. A.; Shahnawaz, M.; Taneja, P.; Dar, M. A. Recent advances in main group coordination driven porphyrins: a comprehensive review. ChemistrySelect 2024, 9, e202304817.

32. Doluca, O.; Withers, J. M.; Filichev, V. V. Molecular engineering of guanine-rich sequences: Z-DNA, DNA triplexes, and G-quadruplexes. Chem. Rev. 2013, 113, 3044–3083.

33. Shimizu, S. Recent advances in subporphyrins and triphyrin analogues: contracted porphyrins comprising three pyrrole rings. Chem. Rev. 2017, 117, 2730–2784.

34. Simbine-Ribisse, E. O.; Fumo, W. C.; Sitoe, E. d. P. E.; Braga, P. A. d. C.; Macuamule, C. J.; Bragotto, A. P. A. Trends on strategies for mitigation of antibiotic residues in milk and dairy products based on scientometric analysis and systematic review. Compr. Rev. Food Sci. Food Saf. 2026, 25, e70398.

35. Noor, H.; David, I. G.; Jinga, M. L.; Popa, D. E.; Buleandra, M.; Iorgulescu, E. E.; Ciobanu, A. M. State of the art on developments of (bio)sensors and analytical methods for rifamycin antibiotics determination. Sensors 2023, 23, 976.

36. Pal, A.; Barkale, H. V.; Dey, N. Dual-mode ratiometric ESIPT probes for vapor-phase detection of a pulmonary agent: leveraging machine learning for high-precision quantitative analysis. Chem. Asian J. 2025, 20, e202401676.

37. Pise, S.; Chatterjee, A.; Dey, N. Exploring self-assembly and viscoelastic behavior of pyrene-based fluorescent hydrogel: designing paper sensors for water-soluble explosives. Eur. J. Org. Chem. 2025, 28, e202401096.

38. Pise, S.; Ahmad, I.; Dey, N. Can conformational flexibility influence the self-assembly behavior and sensing efficacy of fluorogenic amphiphiles? A case study with bisbenzimidazole-based probes. Anal. Methods 2025, 17, 1137–1147.

39. Pal, A.; Mondal, S.; Sharma, R.; Dey, N. Trace-level moisture detection in soil and leaves: integrated machine-learning assisted optical sensing with smart phone enabled digital colorimetry. Mater. Today Chem. 2025, 48, 102891.

40. Barkale, H. V.; Narayn, A.; Polumati, G.; Sahatiya, P.; Dey, N. Stimuli-responsive reversible band-gap engineering: application of oligo(p-phenylenevinylene) derivatives for visible-light-driven photodetector applications. ACS Appl. Electron. Mater. 2025.

DOI: 10.1039/D6SD00054A

Structure-Guided Aggregation-Regulated and Coordination-Assisted Zn–Porphyrins for Decoding Aminoglycoside Recognition in Real-Life Samples

Nisha Chettri,[a±] Harshal V Barkale,[b±] Satadru Jha,[a] Nilanjan Dey[b*]

[a] Department of Chemistry, Sikkim Manipal Institute of Technology, Sikkim Manipal University, Majitar, Sikkim 737136, India.

[b] Department of Chemistry, BITS-Pilani Hyderabad Campus, Shameerpet, Hyderabad-500078, Telangana, India, *Email: nilanjandey.iisc@gmail.com

±Both the authors contributed equally to this work

The Data will be available from authors on reasonable request